Current Topics in Catalysis
Vol. 13, 2017

Mini-Review

Seriatim ECSTM-DEMS of Cu-catalyzed reduction of CO in alkaline solution: *Operando* correlation of electrode-surface atomic structure with product selectivity

Youn-Geun Kim[1], Alnald Javier[2], Jack H. Baricuatro[1] and Manuel P. Soriaga[2,*]
Joint Center for Artificial Photosynthesis, [1]Division of Chemistry and Chemical Engineering; [2]Division of Engineering and Applied Science, California Institute of Technology, Pasadena, CA 91125, USA.

ABSTRACT

Copper is the only unalloyed metal that can deliver, in a "one-pot" heterogeneous electrochemical reduction of CO_2, a remarkable variety of products, up to fifteen hydrocarbons and oxygenates, in different yields. Its overall activity may be substantial, but its selectivity is far from desirable. In the production of liquid fuels, Cu generates only ethanol at nominal efficiencies that depend upon the particular electrode-surface structure. The optimization of ethanol production may be aided by the correlation, under actual reaction conditions, between the atomic structures of the Cu surfaces and their respective product selectivities. Such *operando* correlation is made possible by the *seriatim* (sequential) application of electrochemical scanning tunneling microscopy (ECSTM) and differential electrochemical mass spectrometry (DEMS). The present quasi-review paper describes how *seriatim* ECSTM-DEMS was utilized to show that ethanol is generated exclusively, *sans* other hydrocarbons and oxygenates, by a stepped Cu(S)-[3(100)×(111)], or Cu(511), surface at appreciably low overvoltages.

KEYWORDS: electrochemical scanning tunneling microscopy (ECSTM), Cu-catalyzed electrochemical reduction of CO_2, differential electrochemical mass spectrometry (DEMS), *seriatim* ECSTM-DEMS, Cu(S)-[3(100)×(111)] or Cu(511) stepped surfaces.

*Corresponding author: msoriaga@caltech.edu

INTRODUCTION

The electrochemical reduction of carbon dioxide directly to valued products such as liquid fuels is an exceptionally difficult proposition because the conversion is both thermodynamically and kinetically unfavorable [1-9]. Whereas the power requirements may be mitigated by the use of solar energy, as done in artificial photosynthesis [10-14], the resolution of the torpid reactivity is a much more onerous aspiration since a catalyst is required that significantly enhances both the activity and the selectivity. Copper is the only unalloyed metal known to catalyze the production of a remarkable variety of compounds, albeit at rather different yields [1, 2, 15-23]. The commercial use of Cu electrocatalysts is presently obstructed, however, because the overall energy-conversion efficiency, the ratio of the free energy of the products to that consumed in the reaction, is less than 40%; furthermore, at a benchmark current density of 5 mA cm^{-2}, the overpotential at Cu remains unacceptably large at *ca*. -1.1 V [1, 2, 15, 17]. The analytical separation of multiple products also introduces unwelcome analytical challenges, especially when only one product is desired.

The simplest of liquid fuels that can be obtained from CO_2 reduction (CO_2R) are methanol and ethanol. On Cu electrodes, CH_3OH is produced in

only minuscule amounts, and, although CH_3CH_2OH is generated in much larger quantities, the yield is five times lower than those for gaseous products such as methane and ethylene. It is known that heterogeneous catalytic reactions are influenced by the atomic structure of the catalyst surface. Hence, insights into the preferential generation of ethanol may be obtained by a direct correlation, under reaction (*operando* [24, 25]) conditions, between the product selectivity and the structure of the active Cu electrode. Product distribution can be conveniently determined by differential electrochemical mass spectrometry (DEMS) [26, 27], while the *operando* surface structure can be monitored by electrochemical scanning tunneling microscopy (ECSTM) [28]; the structure-selectivity correlation can be extracted from the sequential application of the two techniques; that is, *seriatim* ECSTM-DEMS [29, 30]. The unbearably low production of methanol, however, strongly suggests that an alternative electrocatalyst, not necessarily copper-based, may have to be sought. In this regard, a theory-directed search for a better methanol-selective material becomes imperative. The new catalyst would most likely be an alloy since no single metal behaves better than elemental copper; this is in line with a set of purported "CO_2R thumb rules" for the production of pure and oxygen-substituted hydrocarbons[†]. The search protocol for a methanol-selective catalyst is beyond the scope of the present article.

The absence of *operando* options in surface structural determinations is not a trivial issue because, under CO_2R/COR conditions, Cu undergoes surface reconstruction, as recently revealed in ECSTM experiments: When an electropolished polycrystalline Cu [Cu(pc)] electrode was held at -0.9 V (SHE) in 0.1 *M* KOH, the surface underwent sequential reconstruction, first to a Cu(111) plane and eventually to a Cu(100) surface, the latter designated here as Cu(pc)-[Cu(100)] [28]. The discovery indicated that the surface structures before, during, and after the electrocatalytic reaction are not immutable. The experimental limitation may be remedied by the parallel implementation of ECSTM and DEMS. The present paper describes results from combined ECSTM-DEMS that made possible the identification of the unique Cu surface structure that catalyzes the reduction of CO exclusively to C_2H_5OH at low overpotentials.

[†]With respect to the selective generation of hydrocarbons and alcohols: (i) No metal shows better activity than Cu. (ii) Alloys do not enhance activity but may improve selectivity. (iii) Catalytic activity can be increased, but at the expense of selectivity, and vice-versa. (iv) It is best if $\Delta G_{H,ads}$ and $\Delta G_{CO,ads}$ were not too different from one another; for Cu, the ratio of $\Delta G_{H,ads}$ to $\Delta G_{CO,ads}$ is close to unity. (v) Selectivity can be regulated by an atomic-level control of surface structure. (vi) Under CO_2R conditions, surfaces may undergo surface reconstructions that can alter both activity and selectivity.

EXPERIMENTAL METHODS

Ample description of the empirical methodologies employed in the present study, *viz*., electrochemistry, ECSTM, DEMS, and monolayer-limited $Cu \leftrightarrow Cu_2O$ oxidation-reduction cycles (ORC), is provided in the 'Supplementary Information (SI)' below. The purpose of the multiple ORC was to induce minor but controllable surface transformations and determine whatever influences are imparted on the product distribution.

RESULTS AND DISCUSSION

Figure 1A shows a steady-state cyclic voltammogram (CV) of a well-ordered Cu(100) electrode surface that had been held at -0.9 V (SHE) in 0.1 *M* KOH for sixty minutes; the CV scans were conducted while the electrode was inside the STM cell so that ECSTM images could be obtained at the same time. As described elsewhere [31], the anodic peak at 0.03 V represents the monolayer-limited formation of surface cuprous oxide, $2Cu_{(s)} + H_2O \rightarrow Cu_2O_{(s)} + 2e^- + 2H^+$, whereas the cathodic peak at -0.4 V is for the reduction of $Cu_2O_{(s)}$ back to elemental copper. No distinctive images could be acquired at potentials more positive than -0.6 V because cuprous oxide starts to form and, even at residual surface concentrations, proper engagement of the STM tip is already hindered. More negative potentials are likewise inaccessible by ECSTM because of deleterious interferences by the hydrogen-evolution reaction.

As previously discussed [29], the image of the Cu(100) plane at -0.9 V is not that of a surface roughened by or littered with isolated islands. This is best elucidated by the progressive low-to-high-resolution images in Figure S1 of the SI. The ECSTM images indicate that the surface consists

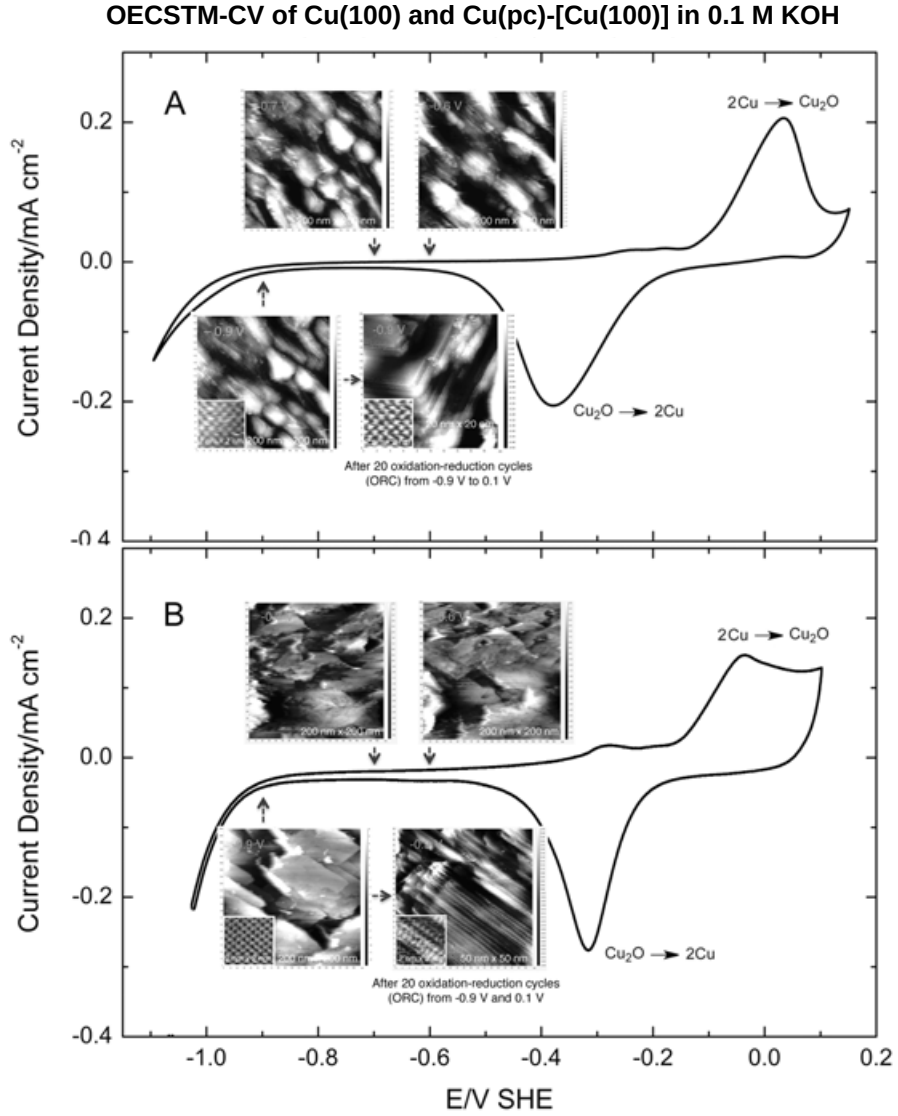

Figure 1. Simultaneous *operando* ECSTM (OECSTM) and cyclic voltammetry (CV) of (A) a well-defined Cu(100) single-crystal surface in 0.1 M KOH solution, before and after multiple oxidation-reduction cycles between 0.1 V and -0.9 V; (B) a polycrystalline copper electrode, Cu(pc), after reconstruction at -0.9 V in 0.1 *M* KOH to a well-defined Cu(100) single-crystal surface, Cu(pc)-[Cu(100)], before and after multiple ORC. The ECSTM images were obtained while the voltammetric plots were being acquired. The geometric area of the single crystal was 1.0 cm^2, and the potential sweep rate was 50 mV s^{-1}.

of sub-micron-sized Cu(100) domains each composed of *ca*. 20-nm-wide terraces segregated by monoatomic steps. The terraces are relatively narrow because the Cu single crystal had not been previously thermally annealed; however, the (100) arrangement of the terrace surface atoms is easily discerned in the image of the 10-nm square section. The zoomed-in atom-resolved (2 nm × 2 nm) ECSTM image shown in the inset of Figure 1A at -0.9 V reveals a highly ordered square (1×1) lattice; the interatomic distance was measured to be 0.27 ± 0.01 nm, a value identical to that of a pristine, oxide-free square Cu(100) net [32].

The data in Figure 1A indicate that no drastic changes in the ECSTM images occurred when the applied potential was increased from -0.9 V to -0.7 V to -0.6 V, or decreased vice-versa. That is, within the potential regime where neither oxide

nor hydride exists on the surface, an ordered Cu(100) exhibited exceptional stability. More remarkable perhaps was the resiliency of the Cu(100) single-crystal surface, as manifested by the fact that numerous voltammetric excursions into the monolayer-limited cuprous-oxide-formation region failed to disrupt the highly ordered atomic arrangement at the terraces (*cf*., pre-ORC and post-ORC images at -0.9 V of Figure 1A). As was first established in an earlier work, a clean and well-ordered Cu(100)-(1×1) surface can be regenerated by simple cathodic reduction of the Cu_2O selvedge [31]. It is also important to mention that the voltammetric anodic and cathodic peaks were identical for the first and twentieth cycles, a result which signifies that the Cu(100) surface was unroughened by the monolayer-restricted ORC. Further corroboration is provided by the root-mean-square roughness, R_{RMS}, of 0.02 nm for the 5 nm × 5 nm ECSTM image (*cf*., *SI*). The roughness factor, R_F, may thus be taken as essentially unity, even after multiple ORC.

The corresponding ECSTM-CV for the reconstructed Cu(pc)-[Cu(100)] electrode surface [29] is shown in Figure 1B. The morphology of the CV is somewhat different from that of the original Cu(100) electrode: (a) The small anodic wave at *ca*. -0.3 V is slightly more pronounced, (b) the Cu-to-Cu_2O oxidation is broader and only slowly recedes to near-zero current, and (c) the Cu_2O-to-Cu reduction peak is noticeably sharper. For the ECSTM images, the dissimilarities are more notable: (i) The terraces are much wider for the reconstructed Cu(pc)-[Cu(100)] surface; nevertheless, the atom-resolved (2 nm × 2 nm) image at -0.9 V reveals that the wide terraces, just like the narrower original Cu(100) terraces, are populated solely by square (100)-arranged atoms. (iii) The sizes of the terraces in the images at -0.7 V and -0.6 V are slightly smaller than at -0.9 V, but still larger than those for the original Cu(100) surface. (iv) In the most significant difference, the post-ORC image for Cu(pc)-[Cu(100)] is no longer the same as that for pure Cu(100). (vi) Based upon the ORC-independent sizes of the redox peaks in Figure 1B, as well as the minimal ECSTM R_{RMS} values, the reconstructed Cu(pc)-[Cu(100)] surface can still be considered atomically smooth.

Figure 2 showcases the results from the implementation of sequential or *seriatim* ECSTM-DEMS for the generation of ethanol at (A) a post-ORC original Cu(100), (B) a pre-ORC reconstructed Cu(pc)-[Cu(100)], and (C) a post-ORC Cu(pc)-[Cu(100)]. At the top of each figure are shown DEMS data in terms of the time-dependence of the ion current for C_2H_5OH at the mass-to-charge ratio (m/z) of 31; at the bottom are the associated ECSTM images. The arrows signify the potentials at which the DEMS and ECSTM measurements were conducted. It first needs to be pointed out that: (i) The ECSTM and DEMS measurements were undertaken separately, but in parallel, since it is obvious that each had to be performed in its own apparatus; to mitigate divergences, the sources, the surface preparations, and the electrochemical pretreatments of the electrodes prior to the experiments were carried out identically. (ii) The ECSTM images displayed were acquired at -0.9 V, and not at -1.0 V, because, at the latter potential, inferior images emerged due to the hydrogen evolution reaction. However, when the electrodes were brought to a potential of -1.0 V, *sans* ECSTM, and then returned to -0.9 V, no changes were observed in the original images. (iii) The reduction was in 0.1 *M* KOH at a rather low overpotential of -1.0 V (SHE), which is 0.8 V less negative than that required for highly reduced products such as CH_4 or C_2H_4 [1, 2, 15]; the evolution of H_2 gas at this potential was also minimal, as can be seen in Figures 1A and 1B. (iv) Both ethanol and methanol yield ion currents at m/z = 31, but ethanol gives an additional MS signal at m/z = 45. Methanol also has a substantial secondary peak at 32, although in the DEMS apparatus, it is obscured by the large signal from residual oxygen. The absence of methanol was inferred from the observation that the ratio of the ethanol signals at m/z of 31 and 45 was the same as that for a CH_3OH-free C_2H_5OH standard. The signal at m/z = 31 was chosen for DEMS quantification because it has the higher signal-to-noise ratio.

Figure 2A shows that a well-ordered Cu(100) surface does not generate ethanol at low potential in alkaline solutions. As already noted in Figure 1A, multiple ORC treatments were unable to disrupt the well-ordered arrangement of the Cu(100) surface atoms; hence, it comes as no surprise that the post-ORC Cu(100) surface remained catalytically inactive towards ethanol production. The catalytic inertness of the ordered Cu(100) surface was further confirmed

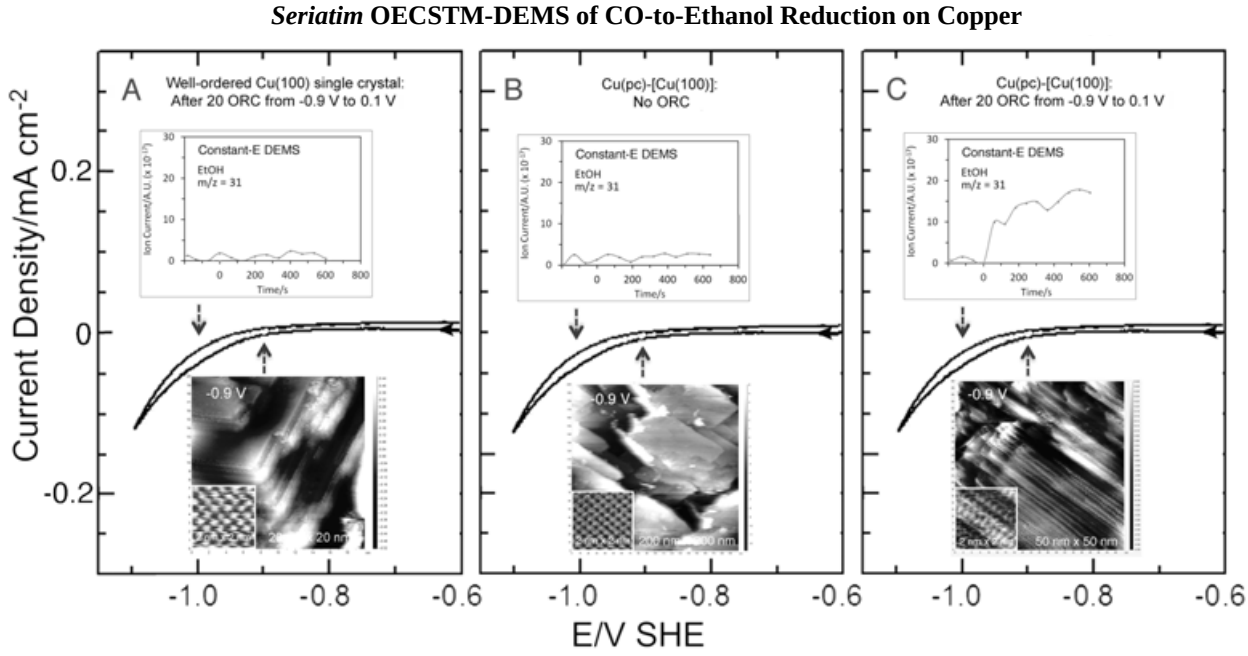

Figure 2. Combined (sequential) ECSTM and DEMS of a 0.1 *M* KOH solution saturated with CO at (A) a well-defined Cu(100) single-crystal after multiple ORC cycles; (B) a reconstructed Cu(pc)-[Cu(100)] without prior ORC; and (C), a reconstructed Cu(pc)-[Cu(100)] after multiple ORC. The potentials for the DEMS and ECSTM measurements are indicated by the arrows. The DEMS signals were only for C_2H_5OH as the product. The ECSTM images were identical before and after potential excursions to -1.0 V; no images could be obtained at that potential because of deleterious effects by the start of the hydrogen evolution reaction.

by the results in Figure 2B which clearly convey the notion that, as long as the reconstructed Cu(pc)-[Cu(100)] is not subjected to oxidation-reduction cycles, it will remain (100)-ordered, and, as a consequence, retain its inability to catalyze the CO-to-C_2H_5OH reduction. On the other hand, the application of multiple ORC on Cu(pc)-[Cu(100)] induced a slight reconstruction to a different, but still ordered, structure grounded largely on the initial Cu(100) motif; as can be seen in the DEMS spectrum in Figure 2C, such a surface generated ethanol.

The quantity of ethanol produced was determined by external calibration in which the MS ion current was plotted as a function of the ethanol concentration in a standard or reference solution. The average concentration of ethanol was found to be 4.0 m*M*, for which the equivalent activity would be 24 μA cm^{-2} based on the electrochemically active surface area estimated from an atomically smooth Cu(100) plane.

The combined ECSTM-DEMS data in Figure 3 provided the evidence that, at appreciably low potential in alkaline solution, the catalytic CO reduction by the post-ORC Cu(pc)-[Cu(100)] surface exclusively favored ethanol as a product over hydrocarbons such as methane and ethylene.

The present investigation offered a definitive atomic-level view of the Cu surface structure associated with the selective reduction of CO to ethanol. The success of the ECSTM experiments was likely abetted by the fact that well-ordered surfaces were employed at the start, and that the perturbations to induce structural transformations were kept to a minimum so as not to stifle the sub-nanometer structural investigations. Figure 4 shows a zoomed-in ECSTM image of the ethanol-product-selective Cu surface; a 5 nm × 5 nm square image is displayed since a 2 nm × 2 nm area would highlight only the terrace but not the step structures. Even a cursory examination of the image promptly reveals a terrace occupied by three rows of Cu(100) atoms and a monatomic step of Cu(111) atoms. The structure is that of a stepped surface, Cu(S)-[3(100)×(111)] or, in shorter notation, Cu(511); the lattice model crystal for such stepped structure is also shown in Figure 4.

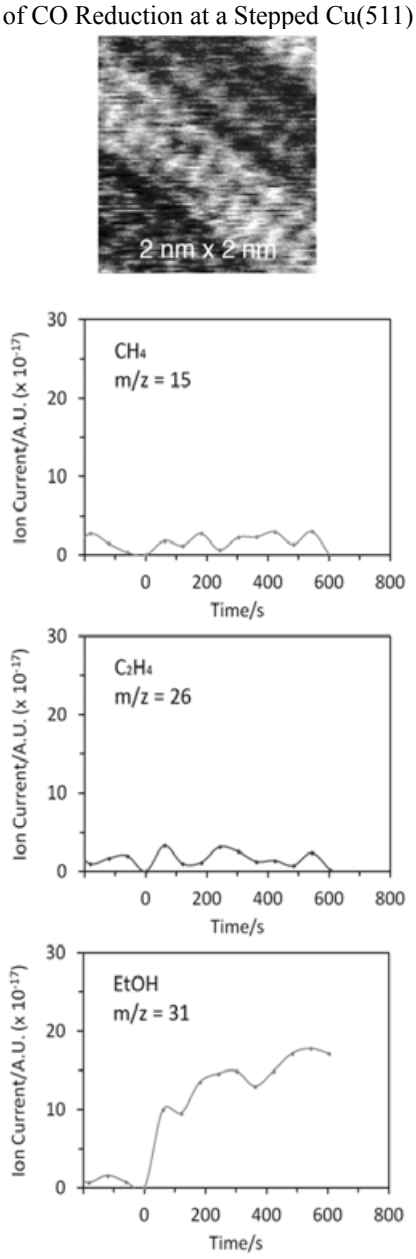

Figure 3. DEMS for a post-ORC reconstructed Cu(pc)-[Cu(100)] at -1.0 V in a 0.1 *M* KOH solution saturated with CO. The DEMS signals were for CH_4, C_2H_4, and C_2H_5OH as products. The post-ORC reconstructed Cu(pc)-[Cu(100)] surface is a stepped Cu(511), or Cu(S)-[3(100)×(111)], surface.

In computational studies on COR or CO_2R mechanisms, Cu(211) is almost always pre-selected as the active stepped surface [3, 4, 6-9], although there appears to be no experimental justification for such a choice. Cu(211) differs from Cu(511) in that the terraces are populated by Cu(111) atoms and the steps by Cu(100); in Cu(511), the terrace and step atoms are Cu(100) and Cu(111), respectively. For the selective CO-to-C_2H_5OH reduction investigated here, the singular role of Cu(511) is almost indisputable: Not only is the Cu(511) structure rather obvious in the ECSTM images, it has also been recently shown that, at a CO_2R potential in 0.1 *M* KOH, a pristine Cu(111) surface reconstructs to Cu(100), but not the other way around [29, 30].

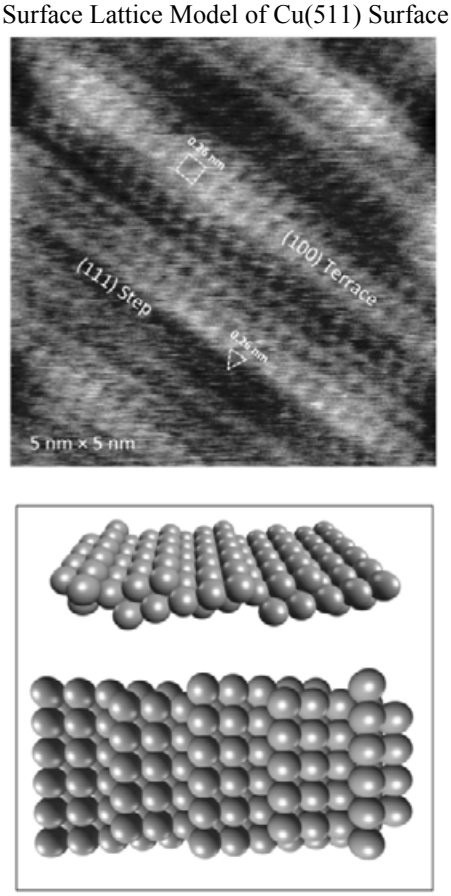

Figure 4. Top: High-resolution ECSTM image of the post-ORC reconstructed Cu(pc)-[Cu(100)] surface that depicts the three-row terrace of Cu(100) atoms and a one-atom step of Cu(111). Bottom: The ideal surface lattice model of the reconstructed Cu(pc)-[Cu(100)] which is a stepped Cu(S)-[3(100)×(111)] or Cu(511) surface.

SUMMARY

The electrocatalytic reduction of CO_2 (or CO) by copper to a variety of products is undesirable if

only one reduced organic compound is sought. The studies described in this paper have provided an example in which, *via* the atomic-level structural alteration of the Cu surface, the product distribution can be regulated to yield only one major compound; experimental measurements made use of *seriatim* ECSTM and DEMS. A pristine and well-ordered Cu(100) surface did not produce ethanol. However, when a Cu(pc)-[Cu(100)] surface, reconstructed from a polycrystalline electrode was further reconstructed *via* mild monolayer-limited $Cu \leftrightarrow Cu_2O$ ORC, the resulting stepped surface, Cu(S)-[3(100)×(111)] or Cu(511), generated only ethanol at a potential 645 mV lower than that which generates multiple products; at the lower potential, neither methane nor ethylene was generated. The combination of ECSTM and DEMS thus paves a path for an *operando* correlation of surface structure and electrocatalytic activity and selectivity.

ACKNOWLEDGMENT

This material is based upon work performed by the Joint Center for Artificial Photosynthesis, a DOE Energy Innovation Hub, supported through the Office of Science of the U.S. Department of Energy under Award No. DE-SC0004993.

SUPPLEMENTARY INFORMATION

Electrochemistry

The electrochemistry experiments for DEMS were conducted with a BioLogic SP-300 potentiostat (BioLogic Science Instruments, Claix, France) equipped for electrochemical impedance spectroscopy (EIS). Potentiostatic EIS measurements were performed at 100 kHz to determine the uncompensated solution resistance (R_u); 85% of R_u was electronically compensated. The potentiostat used for OECSTM was a built-in component of the Agilent 5500 microscope (Agilent Technologies, Santa Clara, CA). All solutions were prepared using 18.2 MΩ-cm Nanopure water (ThermoFisher Scientific, Asheville, NC). Potentials were reported with respect to the standard hydrogen electrode (E_{SHE}) rather than the reversible hydrogen electrode (E_{RHE}); the former was directly relatable to thermodynamic free-energy changes and did not mask pH effects. The interconversion between E_{SHE} and E_{RHE} is given by the equation: $E_{SHE} = E_{RHE} - 0.059$ pH.

Electrochemical scanning tunneling microscopy

The electrochemical cell used for STM was custom-crafted from Kel-F (Emco Industrial Plastics, Inc., Cedar Grove, NJ) fitted with a Pt counter electrode and a pre-calibrated Pt pseudoreference electrode [33]. The STM tips were prepared by an electrochemical etch of a 0.25 mm diameter tungsten wire (Sigma-Aldrich, St. Louis, MO) in 0.6 *M* KOH at 15 VAC. All images were acquired after polarization for an hour at a constant negative potential (-0.9 V) with a high-resolution scanner in a constant-current mode without post-scan processes such as with high-pass filters. A 99.99% Cu disk (GoodFellow, Coraopolis, PA), 10 mm in diameter and 0.5 mm thick, served as the working electrode. Prior to use, the disk electrode was metallographically polished to a mirror finish with a suspension of polycrystalline diamond (Buehler, Lake Bluff, IL) at a grain size of 0.05 μm. The disk was electropolished in 85% H_3PO_4 (Sigma-Aldrich) at 2.0 V for 10 s with a Pt counter electrode; it was then ultrasonicated in, and later rinsed with, deaerated Nanopure water. The polished sample, however, was not thermally annealed. The alkaline solution, 0.1 *M* KOH, used in this study was prepared from analytical-grade KOH reagent (Sigma-Aldrich); it was purged for at least 1 h in oxygen-free, ultrahigh purity argon (Airgas, Radnor, PA).

The root mean square roughness (R_{RMS}) was calculated, with the use of the WSxM software [34], from the surface height data, z_i, obtained from multiple OECSTM images of a given size (e.g., 200 nm × 200 nm or 50 nm × 50 nm). R_{RMS} is an amplitude parameter for roughness, defined in the equation: $R_{RMS} = \left[\frac{1}{N}\sum_{i=1}^{N}|z_i - \bar{z}|^2\right]^{1/2}$; it describes vertical deviations from the mean height $\bar{Z}$. It is important to note that R_{RMS} is a function of the size of the ECSTM image. For a 200 nm × 200 nm image, for example, R_{RMS} was 1.8 nm; for 50 nm × 50 nm, R_{RMS} was 0.2 nm, and, for 5 nm × 5 nm, R_{RMS} was 0.02 nm. The latter value is a more realistic depiction of atomic smoothness since it presents the finest (atomic-level) irregularities. The R_{RMS} for the larger (200 nm × 200 nm) segment represents the waviness, or the more widely spaced deviations, of a surface from its nominal shape [35].

Differential electrochemical mass spectrometry

The general principles of DEMS, along with applications to electrochemical surface science, have been amply discussed elsewhere [36, 37] and will not be repeated here. The disk electrodes used in the DEMS experiments consisted of (i) a 99.99%-pure polycrystalline Cu disk (Goodfellow, Coraopolis, PA), 1.0 cm in diameter and 0.15 mm in thickness, and (ii) a commercially oriented 1.0-mm-thick Cu(100) single crystal, 1.0 cm in diameter and 99.9999% in purity (Princeton Scientific Corp., Easton, PA). Prior to use, the electrodes were metallographically polished and then electropolished for 10 s in 85% phosphoric acid solution (Sigma-Aldrich, St. Louis, MO) at 2.1 V in a two-electrode configuration with a 99.8%-pure graphite rod (Alfa Aesar, Ward Hill, MA). After a thorough rinse in Nanopure water, a potential of -0.90 V was applied to the Cu electrode in a N_2-saturated 0.1 M KOH solution (Sigma-Aldrich) for 2 hours to quantitatively reduce all surface Cu_2O to metallic copper; a 99.99%-pure Pt wire Goodfellow) was used as the counter electrode. Additional purposeful surface structural modifications, such as Cu(pc)-[Cu(100)] reconstruction, followed the procedures outlined above for the OECSTM studies.

The discretely prepared Cu electrode, with a protective layer of electrolyte, was then transferred to the DEMS cell fabricated out of polyether ether ketone, as described previously [26, 27]. A 20-μm-thick polydimethylsiloxane (PDMS) membrane with 20-nm porosity isolated the electrochemical cell from the mass spectrometry compartment, and a 50-μm glass spacer separated the Cu electrode from the PDMS membrane that resulted in a thin-layer electrochemical cell with a volume of 5.0 μL. A porous glass frit placed between the Cu cathode and Pt anode electrodes precluded the oxidation of the CO-reduction products. The potential of the Cu electrode was held at -1.0 V for 600 s while the reduction products were monitored by an HPR-20 quadrupole mass spectrometer (Hiden Analytical, Warrington, England) with a secondary electron multiplier (SEM) detector with a voltage of 950 V and an emission current of 50 μA.

It must be noted that, in DEMS, products that are hydrophobic and volatile can be readily monitored; hence, methane is easily detectable, but species such as acetates cannot be assayed.

Surface oxidation-reduction cycles

Prior to the combined ECSTM and DEMS experiments, the ordered electrodes were subjected to mild (monolayer-limited) oxidation-reduction cycles (ORC) via multiple voltammetric scans, at 50 mV s^{-1}, between 0.1 V and -0.9 V. The intent was to induce controllable surface transformations and determine whatever influences are imparted on the product distribution. At 0.1 V, a single layer of copper(I) oxide, Cu_2O, was formed; at -0.9 V, the surface oxide was reduced back to Cu [31]. Excursions to higher potentials were expected to yield multilayers of copper(II) oxide, CuO, that, upon reduction, would lead to extensive surface roughness that then precluded ECSTM experiments [28]. In contrast, the chosen potential window for the present ORC treatment induced critical structural transformations discernible by ECSTM.

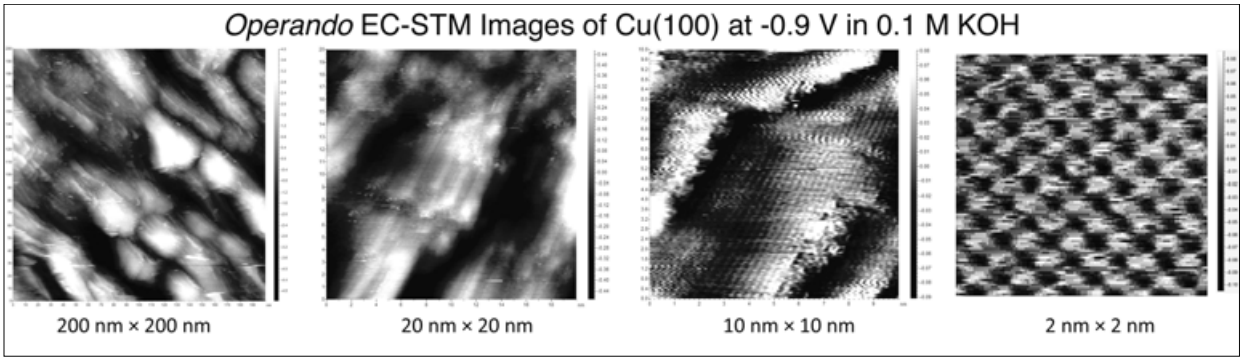

Figure S1. OECSTM images, progressively increased in resolution, of the Cu(100) single-crystal electrode held at -0.90 V (SHE) in 0.1 *M* KOH for 60 minutes. Experimental conditions were as in Figure 1.

CONFLICT OF INTEREST STATEMENT

None of the authors have any conflicts of interest to declare.

REFERENCES

1. Hori, Y. 2008, Modern Aspects of Electrochemistry, C. G. Vayenas, R. E. White and M. E. Gamboa-Aldeco (Eds.), Springer, New York, 89.
2. Kuhl, K. P., Cave, E. R., Abram, D. N. and Jaramillo, T. F. 2012, Energy Environ. Sci., 5, 7050.
3. Chan, K., Tsai, C., Hansen, H. A. and Nørskov, J. K. 2014, ChemCatChem., 6, 1899.
4. Montoya, J. H., Shi, C., Chan, K. and Nørskov, J. K. 2015, J. Phys. Chem. Lett., 6, 2032.
5. Cheng, T., Xiao, H. and Goddard, W. A. 2015, J. Phys. Chem. Lett., 6, 4767.
6. Durand, W. J., Peterson, A. A., Studt, F., Abild-Pedersen, F. and Nørskov, J. K. 2011, Surf. Sci., 605, 1354.
7. Montoya, J. H., Peterson, A. A. and Nørskov, J. K. 2013, ChemCatChem., 5, 737.
8. Peterson, A. A. and Norskov, J. K. 2012, J. Phys. Chem. Lett., 3, 251.
9. Peterson, A. A., Abild-Pedersen, F., Studt, F., Rossmeisl, J. and Norskov, J. K. 2010, Energy Environ. Sci., 3, 1311.
10. Marshall, J. 2014, Nature, 510, 22.
11. Concepcion, J. J., House, R. L., Papanikolas, J. M. and Meyer, T. J. 2012, Proc. Natl. Acad. Sci. USA, 109, 15560.
12. Faunce, T., Styring, S., Michael R. Wasielewski, M. R., Brudvig, G, W., Rutherford, A. W., Messinger, J., Lee, A. F., Hill, C. L., deGroot, H., Fontecave, M., MacFarlane, D. R., Hankamer, B., Nocera, D. G., Tiede, D. M., Dau, H., Hillier, W., Wang, L., Amal, R. 2013, Energy Environ. Sci., 6, 1074.
13. Tachibana, Y., Vayssieres, L. and Durrant, J. R. 2012, Nat. Photonics, 6, 511.
14. Gust, D., Moore, T. A. and Moore, A. L. 2009, Acc. Chem. Res., 42, 1890.
15. Gattrell, M., Gupta, N. and Co, A. 2006, J. Electroanal. Chem., 594, 1.
16. Whipple, D. T. and Kenis, P. J. A. 2010, J. Phys. Chem. Lett., 1, 3451.
17. Schouten, K. J. P., Kwon, Y., van der Ham, C. J. M., Qin, Z. and Koper, M. T. M. 2011, Chem. Sci., 2, 1902.
18. Schouten, K. J. P., Qin, Z., Gallent, E. P. and Koper, M. T. M. 2012, J. Am. Chem. Soc., 134, 9864.
19. Calle-Vallejo, F. and Koper, M. T. M. 2013, Angew. Chem. Int. Ed., 52, 7282.
20. Hori, Y., Takahashi, I., Koga, O. and Hoshi, N. 2002, J. Phys. Chem. B, 106, 15.
21. Hori, Y., Takahashi, R., Yoshinami, Y. and Murata, A. 1997, J. Phys. Chem. B, 101, 7075.
22. Hori, Y., Murata, A., Takahashi, R. and Suzuki, S. 1987, J. Am. Chem. Soc., 109, 5022.
23. Hori, Y., Takahashi, I., Koga, O. and Hoshi, N. 2003, J. Mol. Catal. A: Chem., 199, 39.
24. Bañares, M. A. 2005, Catal. Today, 100, 71.
25. Weckhuysen, B. M. 2002, Chem. Commun., 97.
26. Javier, A., Baricuatro, J. H., Kim, Y.-G. and Soriaga, M. P. 2015, Electrocatalysis, 6, 493.
27. Javier, A., Baricuatro, J. H., Kim, Y.-G. and Soriaga, M. P. 2015, Electrocatalysis, 6, 127.
28. Kim, Y.-G., Baricuatro, J. H., Javier, A., Gregoire, J. M. and Soriaga, M. P. 2014, Langmuir, 30, 15053.
29. Kim, Y.-G., Javier, A., Baricuatro, J. H. and Soriaga, M. P. 2016, Electrocatalysis, 7, 391.
30. Kim, Y.-G., Javier, A., Baricuatro, J. H. and Soriaga, M. P. 2016, J. Electroanal. Chem., 780, 290.
31. Kim, Y.-G. and Soriaga, M. P. 2014, J. Electroanal. Chem., 734, 7.
32. Wyckoff, R. W. G. 1963, Crystal Structures, Wiley, New York.
33. Itaya, K. 1998, Prog. Surf. Sci., 58, 121.
34. Horcas, I. and Fernbandez, R. 2007, Rev. Sci. Instrum., 78, 013705.
35. Vorburger, T. V. 1992, Methods for Characterizing Surface Topography, D. T. Moore (Ed.), Optical Society of America, Washington, DC, 137.
36. Baltruschat, H. 1999, Interfacial Electrochemistry, A. Wieckowski (Ed.), Marcel Dekker, New York, 577.
37. Baltruschat, H. 2004, J. Am. Soc. Mass Spectrom., 15, 1693.